

Geochemistry of Groundwater in MengXu Area, China

Sadek Younes and Luo Zhao Hui

Department of Environmental Engineering and Water Resources,
School of Environmental Studies, China University of Geosciences,
Wuhan 388, Lumo Road, Wuchang, Wuhan, Hubei, R.P. 430074, China

Abstract: Chemical properties and pollution of water resources were studied in the MengXu town basin that is located in the Guiping city, Guangxi Autonomous Region of the Zhuangs, Southern China. Water quality was characterized according to its major constituents and the geological features of the area. Chemical analysis results indicate that groundwater show wide concentration ranges in major inorganic ions, reflecting complex hydro chemical processes. Groundwater in the studied area is, for the most part, weakly to moderately mineralized and dominated by the calcium (Ca^{2+}) and bicarbonate (HCO_3^-) ions. Within the basin, 2 main different hydro geochemical facies out of 7 have been identified: $\text{Ca-HCO}_3\text{-SO}_4$ and Ca-HCO_3 . The predominant water type of groundwater samples is the Ca-HCO_3 facies in the recharge area and has a tendency toward Mg-HCO_3 and Ca-SO_4 facies along the direction of water flow. The results explained the importance of cation exchange, mineral weathering and anthropogenic activities on groundwater chemistry. Chemical analysis of the groundwater shows that the mean concentration of the cations is of the order $\text{Ca}^{2+} > \text{Na}^+ > \text{Mg}^{2+} > \text{K}^+$, while that for anions is $\text{HCO}_3^- > \text{SO}_4^{2-} > \text{Cl}^- > \text{NO}_3^-$. Statistical analyses indicate positive correlation between the most of pairs of parameters. The dissolution of halite, calcite, dolomite and gypsum explains part of the contained Na^+ , Ca^{2+} , Mg^{2+} , Cl^- , SO_4^{2-} and HCO_3^- , but other processes, such as cation exchange and weathering of aluminosilicates also contribute to the water composition. A comparison of groundwater quality in relation to drinking water quality standards proves that most of the water samples are suitable for drinking water purpose whereas groundwater in some areas of the district has low salinity and low Sodium Adsorption Ratio (SAR), indicating suitability for irrigation water.

Key words: Hydrogeochemistry, groundwater, guiping, hydrochemical facies, hydrochemical process

INTRODUCTION

Increased knowledge of geochemical processes that control groundwater chemical composition in humid karst regions could lead to improved understanding of hydro chemical systems in such areas. Such improved understanding can contribute to management and utilization of the groundwater resource by clarifying relations among groundwater quality, aquifer lithology and recharge type. Groundwater is the primary source of water for human consumption, as well as for agriculture and industrial uses, which make it an important resource in China. Continued population growth in China is rapidly depleting groundwater supplies in some areas. Further, intensive use for irrigation makes groundwater a critical resource for human activities. Sedimentary basins form

important groundwater resources for the MengXu town area, in the South of China. Most of the agricultural plains in MengXu town lie on these rock systems and the problem of groundwater quality deterioration have become urgent, because of the intensive farming and the increasing exploitation of the aquifers and also mining in this area.

The aim of this study, was to determine chemical constituents and the main geochemical reactions, which control the groundwater composition in a Karst aquifer in southern China.

Study area: MengXu town is located in Guiping County with distance of 13 km southwest from the city of Guiping. The study area is about 30 km^2 in the range of $109^\circ 58' 26'' \sim 110^\circ 01' 43'' \text{E}$ and $23^\circ 16' 11'' \sim 23^\circ 19' 00'' \text{N}$ (Fig. 1).

Corresponding Author: Sadek Younes, Department of Environmental Engineering and Water Resources,
School of Environmental Studies, China University of Geosciences, Wuhan 388, Lumo Road,
Wuchang, Wuhan, Hubei, R.P. 430074, China

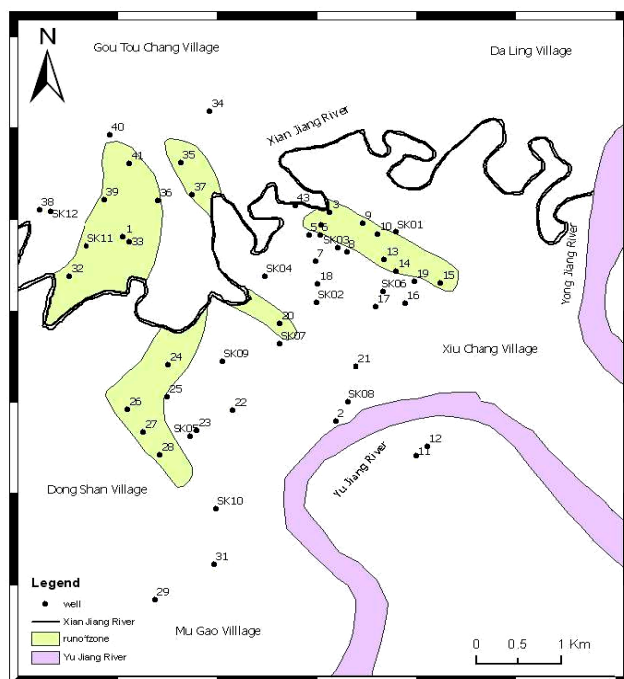


Fig. 1: Study area showing location of wells sampled for groundwater analysis

The climate is subtropical in study area with high temperatures, high humidity, plenty of rainfall. The annual temperature is 21.4°C. Temperature is highest in July with an average of 28.6°C and lowest in January with an average of 12.3°C. According to rainfall data (1953-2001), of Guiping rainfall stations, the average rainfall is 1745.1 mm year⁻¹ and most rainfall concentrates. In April-September.

The study area is mainly plain with low hills in southwest, northwest and southeast parts. The highest hill is Dalingshan in southwest part with elevation of 163.5 m. The main Karst plain is about 35-40 m in elevation. Yujiang River, the largest branch of Zhujiang River, runs in south and east boundary of study area. Xiaojiang River, the only big tributary of Yujiang River in this area, winds from west to east in the center part and pours into Yujiang River near Yongjiang village and so this study area is divided by Xiaojiang River as south part and north part. There are 2 tributaries of Xiaojiang River in this area named Beixiaohe River in north part and Nanxiaohe River in south part.

Bedrocks in the MengXu town basin consist of granites, schist, dolomite, limestone and plagioclase mineral. The schists contain mostly quartz and are micaceous. Black slates are widely distributed in the studied area. Besides these, there are shales, sandstones and marls containing limestone. Soils in the studied area are calcareous.

MATERIALS AND METHODS

Groundwater samples were collected from 41 representative open wells during July 2007 (Fig. 1). Electrical Conductivity (EC) and pH were measured using digital meters immediately after sampling. Two copies for every water sample was collected in the field, one was original water without any treatment and HNO₃ was added in another copy to fix metal ions. All samples were then analyzed in laboratory for chemical constituents, 7 anions in original sample copy were detected by using Ion Chromatograph (IC) and other cations were detected by ICP-MS (Table 1).

RESULTS AND DISCUSSION

Hydro chemical facies: The water types in the area of study were determined based on their chemical composition. Chemical analyses were plotted on a Piper diagram (Fig. 2).

The Piper triangular diagram is useful for evaluating the geochemical evolution of the groundwater that not only shows the chemical character of each water sample, but also the relationship between samples. It was constructed using Aquachem Software show mainly a typical Ca-HCO₃ and Ca-HCO₃-SO₄ chemical facies. They are weakly mineralized and have a near neutral pH.

Ground waters in this region are significantly dominated by Ca²⁺, Mg²⁺ and HCO₃⁻. Groundwater quality

Table 1: Chemical analysis data and descriptive analysis of the analyzed chemical components for the study area. (All data in mg L⁻¹ except for EC; $\mu\text{S cm}^{-1}$)

Samples	PH	EC	Ca-43	K-39	Mg-24	Na-23	Sr-88	SO ₄ ²⁻	HCO ₃ ⁻	NO ₃ ⁻	Cl-	TDS	SI dolomite	SI calcite	SI gypsum
SD001	7.3	624	59.833	0.636	4.815	4.433	0.199	42.548	151.020	26.373	9.577	306.100	-0.974	-0.114	-1.986
SD002	7.3	302	42.098	1.087	3.035	1.589	0.106	14.747	133.940	7.624	5.791	145.300	-1.343	-0.275	-2.524
SD004	7.9	204	23.727	1.325	4.391	1.189	0.061	13.852	85.733	3.847	5.843	100.800	-0.574	-0.095	-2.746
SD005	7.8	290	37.034	0.854	3.135	0.301	0.082	13.608	134.240	18.173	4.267	141.200	-0.394	0.164	-2.613
SD008	7.8	289	39.448	0.883	3.487	0.593	0.085	12.503	138.520	3.508	5.079	135.200	-0.284	0.210	-2.618
SD009	8.1	195	25.363	0.309	1.732	0.061	0.068	13.357	85.428	2.318	4.028	90.100	-0.551	0.132	-2.722
SD014	8.1	210	23.924	1.529	2.277	0.201	0.072	12.047	92.445	3.161	4.864	92.800	-0.392	0.140	-2.795
SD017	7.9	239	48.417	1.660	1.800	0.441	0.110	27.219	122.960	2.828	8.245	165.000	-0.415	0.333	-2.210
SD021	7.3	255	40.882	0.586	1.591	0.402	0.080	10.728	130.580	2.512	3.176	126.500	-1.637	-0.288	-2.657
SD024	7.2	190	30.461	0.772	1.308	0.929	0.069	8.914	100.990	2.475	3.834	100.200	-2.234	-0.608	-2.828
SD028	7.1	322	35.020	3.764	2.454	0.831	0.107	24.810	119.600	3.944	8.675	132.800	-2.004	-0.599	-2.363
SD029	7.8	373	31.380	5.019	2.970	0.836	0.110	27.667	96.107	--	10.017	126.300	-0.757	-0.040	-2.351
SD035	7.6	310	43.928	1.759	1.924	0.418	0.104	26.583	112.080	3.093	7.733	149.000	-1.084	-0.037	-2.249
SD039	7.4	380	63.326	1.076	2.913	0.165	0.127	41.097	150.720	2.900	9.088	280.700	-0.949	0.020	-1.960
SD043	7.5	266	38.464	1.007	1.084	0.040	0.088	30.251	82.072	1.967	11.344	173.600	-1.840	-0.319	-2.229
SD047	8.2	323	43.885	2.479	1.429	0.684	0.129	54.478	59.495	3.982	19.993	197.300	-0.614	0.263	-1.949
SD049	7.2	352	34.629	6.915	1.894	1.342	0.107	41.263	71.088	2.849	17.053	145.300	-2.379	-0.731	-2.145
SD052	8.1	151	28.135	0.650	0.996	1.753	0.073	19.045	60.105	2.535	4.563	121.500	-1.053	0.025	-2.524
SD056	7.8	317	31.904	1.165	1.751	0.083	0.103	28.389	123.570	3.122	7.904	111.800	-0.774	0.069	-2.339
SD058	7.2	300	41.795	3.340	2.900	1.617	0.104	65.481	46.070	2.426	11.194	179.200	-2.521	-0.853	-1.889
SD062	7.3	275	40.357	1.204	1.522	2.482	0.114	6.843	42.714	38.650	26.581	162.800	-2.636	-0.781	-2.865
SD069	7.3	377	73.908	0.687	3.077	2.128	0.117	21.999	171.160	3.237	7.544	283.100	-0.946	0.043	-2.176
SD072	8.6	137	15.670	0.314	1.526	1.824	0.054	14.174	47.596	2.015	2.549	55.100	-0.322	0.169	-2.866
SD077	7.8	220	32.224	0.274	1.317	1.052	0.069	8.116	110.750	2.628	2.919	95.400	-0.946	0.047	-2.853
SD080	7.1	95	6.856	1.143	1.196	3.023	0.035	10.498	33.256	3.499	3.243	35.900	-3.990	-1.789	-3.306
SD083	5	458	75.629	0.039	7.759	2.259	0.132	155.750	67.427	2.382	2.194	311.800	-6.041	-2.697	-1.376
SD085	7.2	306	48.989	0.764	3.722	0.637	0.094	34.019	113.190	3.092	4.042	208.800	-1.557	-0.392	-2.115
SD086	7.2	140	21.001	0.191	1.739	1.416	0.047	4.510	72.919	1.955	2.178	65.000	-2.510	-0.888	-3.245
SD093	7.5	351	30.300	1.810	4.957	0.745	0.062	19.181	91.530	2.179	6.214	156.900	-1.171	-0.367	-2.521
SD094	7.5	600	81.763	5.143	7.060	10.630	0.153	74.974	195.570	10.335	50.032	333.500	-0.129	0.294	-1.670
SD096	7.8	340	30.391	1.803	5.450	0.771	0.068	12.531	110.450	3.230	5.702	110.800	-0.376	0.011	-2.709
SD103	7.7	245	46.718	0.178	0.934	0.883	0.078	16.789	106.480	7.846	3.908	183.500	-1.208	0.071	-2.418
SD104	8	293	52.104	0.118	2.301	1.393	0.089	8.564	165.670	6.554	4.467	152.800	0.172	0.588	-2.692
SD108	7.9	286	37.836	0.975	2.663	0.450	0.095	19.474	113.800	2.008	6.882	121.800	-0.386	0.209	-2.434
SD114	8.2	282	45.975	0.284	3.365	0.466	0.088	31.458	94.886	13.130	4.699	194.200	0.187	0.487	-2.174
SD122	7.8	304	74.827	1.030	3.928	1.349	0.111	26.877	197.700	9.365	9.015	324.700	0.253	0.591	-2.102
SD126	7.7	266	39.811	1.183	3.840	0.375	0.078	15.371	118.680	3.018	5.526	188.300	-0.564	0.051	-2.521
SD131	8.2	214	41.023	0.696	1.439	1.387	0.082	18.504	94.581	4.499	3.485	165.000	-0.192	0.456	-2.420
SD135	8	324	64.128	0.138	2.125	0.917	0.095	20.003	180.010	12.577	4.294	283.700	0.257	0.692	-2.269
SD139	8.2	182	28.362	1.113	1.099	1.989	0.076	17.567	67.732	5.340	4.394	126.300	-0.717	0.173	-2.562
SD141	7.5	552	86.125	2.875	7.266	4.746	0.128	32.777	181.230	18.962	19.187	353.700	-0.115	0.305	-1.987
XJ river	8.3	226	23.246	1.987	5.922	1.069	0.059	17.970	62.546	7.253	8.301	0.000	0.044	0.144	-2.650

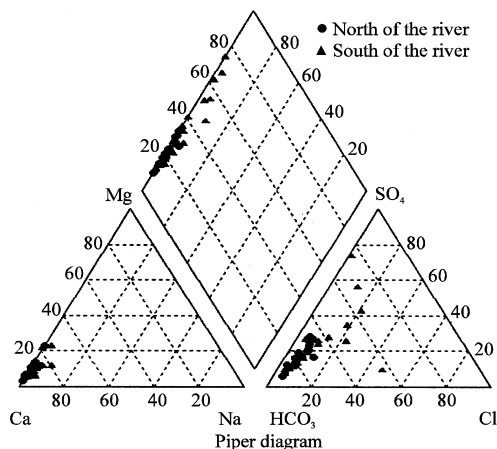


Fig. 2: Diagram of the chemical composition of groundwater samples collected from the area

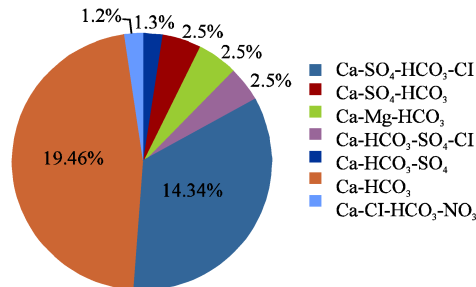


Fig. 3: The average chemical compositions for the water types

sis directly related to the water-rock interaction processes. High HCO₃⁻ and SO₄²⁻ contents are derived from the

carbonate and gypsum contents in the study area but differ from the north and the south part by the residence time. Dissolved solids for the south part are higher than those of the water samples from the north of the Xiao River around the study area. This suggests that the groundwater hydrochemistry is controlled by water-rock interaction and anthropogenic pollution.

Table 2: Concentrations are expressed in mg L⁻¹, TDS in mg L⁻¹ and EC in $\mu\text{S cm}^{-1}$

Samples	EC	Ca-43	K-39	Mg-24	Na-23	Sr-88	SO ₄ ²⁻	HCO ₃ ⁻	TDS	Cl ⁻	NO ₃ ⁻
Min	95.000	6.856	0.039	0.934	0.083	0.035	4.510	33.256	0.000	2.178	1.955
Max	624.000	86.125	6.915	7.759	10.630	0.199	155.750	197.700	353.700	50.032	38.650
Average	294.945	42.382	1.434	2.833	1.515	0.094	26.794	109.129	169.117	8.325	6.403
SD	116.621	17.929	1.474	1.778	2.303	0.030	25.460	42.342	83.384	8.358	7.422

Table 3: The correlation coefficients of the studied parameters

Samples	EC	Ca	K	Mg	Sr	SO ₄ ²⁻	HCO ₃ ⁻	TDS	Cl ⁻	NO ₃ ⁻	Ca+Mg	Ca+Na
EC	1	0.80	0.44	0.76	0.87	0.56	0.61	0.82	0.57	0.42	0.82	0.83
Ca		1	0.22	0.61	0.77	0.54	0.73	0.96	0.46	0.34	1.00	1.00
K			1	0.38	0.34	0.24	0.16	0.24	0.74	0.05	0.24	0.28
Mg				1	0.47	0.59	0.40	0.64	0.37	0.19	0.66	0.63
Sr					1	0.56	0.49	0.79	0.54	0.50	0.76	0.78
SO ₄ ²⁻						1	0.00	0.57	0.29	-0.02	0.56	0.54
HCO ₃ ⁻							1	0.65	0.27	0.16	0.73	0.73
TDS								1	0.46	0.40	0.96	0.96
Cl ⁻									1	0.45	0.46	0.52
NO ₃ ⁻										1	0.34	0.37
Ca+Mg											1	1.00
Ca+Na												1

Based on dominant cations and anions these 7 groups are shown in the following way: Ca-HCO₃-SO₄, Ca-HCO₃ mainly and Ca-HCO₃-SO₄-Cl, Ca-Mg-HCO₃, Ca-SO₄-HCO₃, Ca-SO₄-HCO₃-Cl, Ca-Cl-HCO₃-NO₃. The average percentage chemical compositions for the seven subtypes are given in Fig. 3.

The Ca-SO₄-HCO₃, Ca-Mg-HCO₃ and Ca-HCO₃-SO₄-Cl each represent 2.5% of the total number of water samples analyzed, while Ca-Cl-HCO₃-NO₃ and Ca-SO₄-HCO₃-CL represent 1.3 and 1.2%, respectively. The Ca-HCO₃- and Ca-HCO₃-SO₄ type water is dominated in the most part of studied area around 20 and 15%, respectively in the whole area. The TDS value for the Ca-HCO₃ type is <354 mg L⁻¹ and Ca-SO₄ type (307 mg L⁻¹).

Groundwater quality evolution: The groundwater quality is enough according World Health Organization for the majority of water samples. The majority of samples are within the permissible drinking limits of WHO. Nitrate concentrations in the well samples varied from 1.955-38.65 mg L⁻¹ with the average of 6.403 mg L⁻¹.

In comparison with the WHO's drinking water guideline of 50 mg L⁻¹ for NO₃⁻, all the samples show a low concentration. Changes in groundwater salinity and chemical composition occur in the middle and south of the studied area due to either natural and/or anthropogenic activity (Ritcher and Kreidler, 1993).

The chemical compositions (major elements) in the well waters (41 samples) were represented in the Table 2.

The origin of solutes

Calcite dissolution: The most common weathering reaction for calcite is simple dissolution (Drever, 1988), giving a 1/2 Ca: HCO₃ equivalence ratio of 1:1. Dissolution of carbonate is an equilibrium process, which is controlled

by CO₂ partial pressure. The main sources of CO₂ in the groundwater are adsorption from the atmosphere or from the decomposition of organic matter in the recharge area, of which the latter is the major source. Furthermore, to form bicarbonate by fixation of CO₂, this anion is released by the dissolution of calcite and the weathering of silicate minerals. The abundance of carbonate and dolomite rocks in the basin, suggests that dissolution of these minerals will add significant amounts of Ca²⁺ and Mg²⁺ to the reservoirs. Evaluation of the slopes of Ca²⁺, Mg²⁺ and Na⁺ with HCO₃⁻ gives valuable information about the stoichiometry of the process (Edmunds *et al.*, 1987). Figure 4l shows the relationship between Ca²⁺ and HCO₃⁻ in groundwater. As it can be seen, there is no relationship between these ions and the correlation coefficient is not significant (Table 3). This indicates that calcite is the main source of Ca⁺. Figure 4i shows that most of the data deviated from the expected 1:1 relation indicating another source of Mg²⁺ must be present, possibly from weathering. The origin of the Mg²⁺ must be associated, at least partially, with the dissolution of aluminosilicates. The excess of Mg²⁺ may also, result from dissolution of sodium and magnesium sulfate minerals. Figure 4k shows the value of HCO₃⁻ as a function of Na⁺ in the groundwater samples. As can be seen, most of the groundwater samples deviated from the 1:1 relation, indicating another source of Na⁺.

Gypsum dissolution: Calcium and sulfate ions in groundwater are provided partly by the dissolution of gypsum. A plot of Ca²⁺ and SO₄²⁻ (Fig. 4e) shows that most of the groundwater samples deviated from the 1:1 line, indicating another source of Ca⁺. There was a strong correlation between Mg²⁺ and SO₄²⁻ and Na⁺ and SO₄²⁻ suggesting that most of the SO₄²⁻ originates from

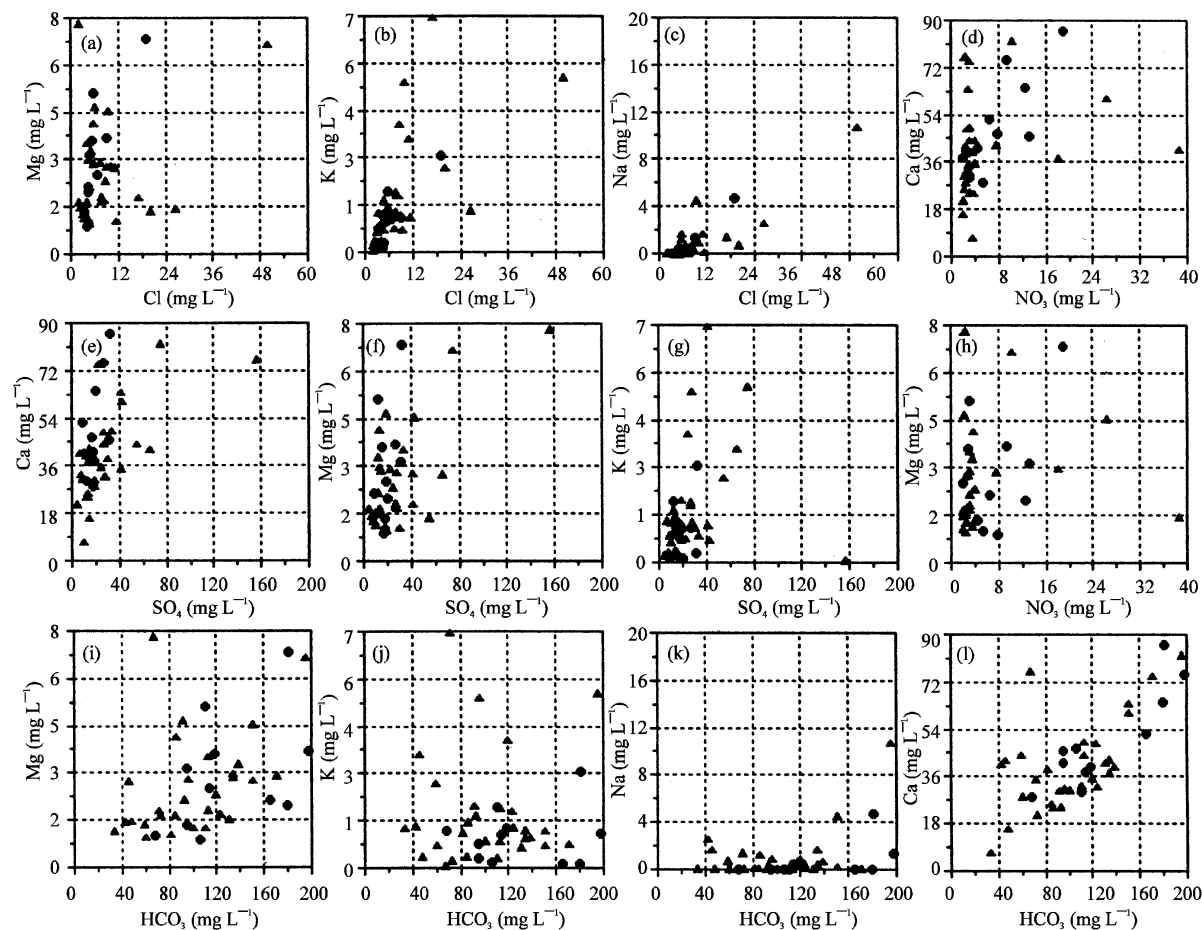


Fig. 4: Relationship between different cations and anions in the groundwater of the studied area

dissolution of sodium and magnesium minerals (Fig. 4f). Therefore, the positive correlation between the above mentioned pairs of cations and anions suggest that these ions are part of a buried evaporate body in the MengXu town basin. Weak correlation between K^+ and other major ions suggest that K^+ is derived mostly from K-feldspars. If Ca^{2+} , Mg^{2+} , SO_4^{2-} and HCO_3^- are derived from simple dissolution of calcite, dolomite and gypsum, then a charge balance should exist between the cations and anions. As indicated in (Fig. 5), a deficiency of $(HCO_3^- + SO_4^{2-})$ relative to $(Ca^{2+} + Mg^{2+})$ exists in most of the groundwater samples.

The ionic relations suggest that Ca^{2+} and Mg^{2+} provided by calcite, dolomite and gypsum dissolution are replaced by Na^+ from a source other than NaCl. The evidence for silicate weathering and/or cation exchange is given by bivariate plots of $Ca^{2+} + Mg^{2+}$ - $HCO_3^- - SO_4^{2-}$ as a function of $Na^+ + K^+ - Cl^-$, as shown in Fig. 6.

Compositional relations among dissolved species can reveal the origin of solutes and the process that generated the observed water compositions. Statistical analyses indicate a positive correlation between some pairs of parameters shown in (Fig. 4) and (Table 3).

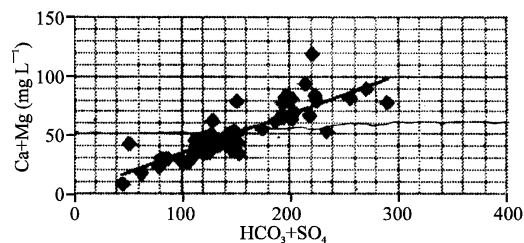
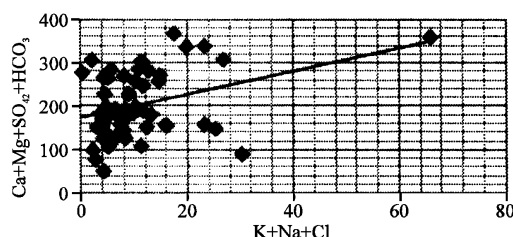


Fig. 5: Relation between $Ca+Mg$ and HCO_3+SO_4 in MengXu town groundwater

The Na-Cl relationship has often been used to identify the mechanisms for acquiring salinity and saline intrusions in semi-arid regions (Magaritz *et al.*, 1981; Dixon and Chiswell, 1992; Sami, 1992). The high Na+ and Cl- contents detected in certain samples may suggest the dissolution of chloride salts. A parallel enrichment in both ions indicates dissolution of chloride salts or concentration processes by evaporation. These 2 mechanisms are those that predominate in the studied region, with a distribution of values very close to one in few cases. Figure 4c shows the value of Cl as a function

Table 4: Quality of irrigation water based on electrical conductivity

EC ($\mu\text{S cm}^{-1}$)	Water class	Representing well	Total no of wells
<250	Excellent	3, 6, 7, 8, 10, 18, 23-25, 28, 32, 38, 40	25
250-750	Good	1, 2, 9, 11-16, 19-22, 26, 27, 29-31, 33-37	13
750-2000	Permissible	Nil	Nil
2000-3000	Doubtful	Nil	Nil
>3000	Unsuitable	Nil	Nil

Fig. 6: Relation between $\text{Ca}+\text{Mg}+\text{SO}_4+\text{HCO}_3$ and $\text{Na}+\text{K}+\text{Cl}$ in MengXu town groundwater

of Na^+ in the groundwater samples. The dissolution of halite or gypsum in water release equal concentrations of sodium and chloride into the solution, but analytical data in (Fig. 4c) deviates from the expected 1:1 relation indicating that a large fraction of sodium is associated with an anion other than chloride. A Na/Cl molar ratio greater than one is typically interpreted as reflecting Na^+ released from silicate weathering reactions (Meybeck, 1987). Silicate dissolution can be a probable source for Na in groundwater in the MengXu town area. The excess of sodium in these samples may also, result from dissolution of sodium sulfate minerals. That sample SD 083 with a value of Na/Cl ratio higher than one show a deficit in $\text{Ca}^{2+}+\text{Mg}^{2+}$ and this is consistent with a $\text{Ca}^{2+}-\text{Na}^+$ cation exchange process, which leads to a softening of the water (Hidalgo and Cruz-Sanjulian, 2001). The contribution of potassium to the groundwater in this sample is modest. The low levels of potassium in natural waters are a consequence of its tendency to be fixed by clay minerals and to participate in the formation of secondary minerals (Mathess, 1982).

Therefore, the excess positive charge of Ca^{2+} and Mg^{2+} must be balanced by Cl^- , the only major anion. In Table 1, the saturation indices for calcite, dolomite and gypsum are shown. The calculations were carried out with the speciation program PHREEQC (Parkhurst and Appelo, 1999). Nearly, all water samples were oversaturated with respect to calcite and dolomite, suggesting that these carbonate mineral phases may have influence on the chemical composition of the study area.

Salinity and alkalinity hazard: Electrical conductivity is a good measure of salinity hazard to crops as it reflects the TDS in groundwater. The 25 out of 38 samples of the study area display an excellent water class (Table 4) for irrigation (Ragunath, 1987). So, there is no excess salinity, which reduces the osmotic activity of plants and thus,

Table 5: Alkalinity hazard classes of groundwater

SAR	Salinity hazard	Water class	Representing well	Total no of wells
<20	S1	Excellent	All wells	38
10-18	S2	Good	Nil	Nil
18-26	S3	Doubtful	Nil	Nil
>26	S4	Unsuitable	Nil	Nil

Table 6: Suitability of groundwater for irrigation based on percent sodium

Na %	Water class	Representing well	Total no of wells
<20	Excellent	All wells	38
20-40	Good	Nil	Nil
40-60	Permissible	Nil	Nil
60-80	Doubtful	Nil	Nil
>80	Unsuitable	Nil	Nil

interferes with the absorption of water and nutrients from the soil (Saleh *et al.*, 1999). Sodium Adsorption Ratio (SAR) is an important parameter for determining the suitability of groundwater for irrigation because it is a measure of alkali/sodium hazard to crops. SAR is defined by Karanth (1989):

$$\text{SAR} = \frac{\text{Na}^+}{(\text{Ca}^{2+} + \text{Mg}^{2+})^{1/2} / 2}$$

Where, the concentrations are reported in meq L^{-1} . The SAR values range from 0.01-1.59 with an average value of 0.29. All Ground- water samples of the study area fall in the low sodium class (S1) (Table 5). This implies that no alkali hazard is anticipated to the crops. If the SAR value is greater than 6-9, the irrigation water will cause permeability problems on shrinking and swelling types of clayey soils (Saleh *et al.*, 1999). The analytical data plotted on the US salinity diagram illustrates that most of the groundwater samples fall in the field of C3 S1, indicating high salinity and low sodium water, which can be used for irrigation on almost all types of soil with little danger of exchangeable sodium (Fig. 7). Few samples fall in the field of C4 S1, indicating very high salinity and low alkalinity hazard. This can be suitable for plants having good salt tolerance and also restricts their suitability for irrigation, especially in soils with restricted drainage (Karanth, 1989; Mohan *et al.*, 2000). The sodium percentage (Na%) is calculated using the formula given below:

$$\text{Na\%} = \frac{(\text{Na}^+ + \text{K}^+)}{(\text{Ca}^{2+} + \text{Mg}^{2+} + \text{Na}^+ + \text{K}^+)} \times 100$$

Where, all the concentrations are expressed in meq L^{-1} . The Na% shows a very good quality of groundwater

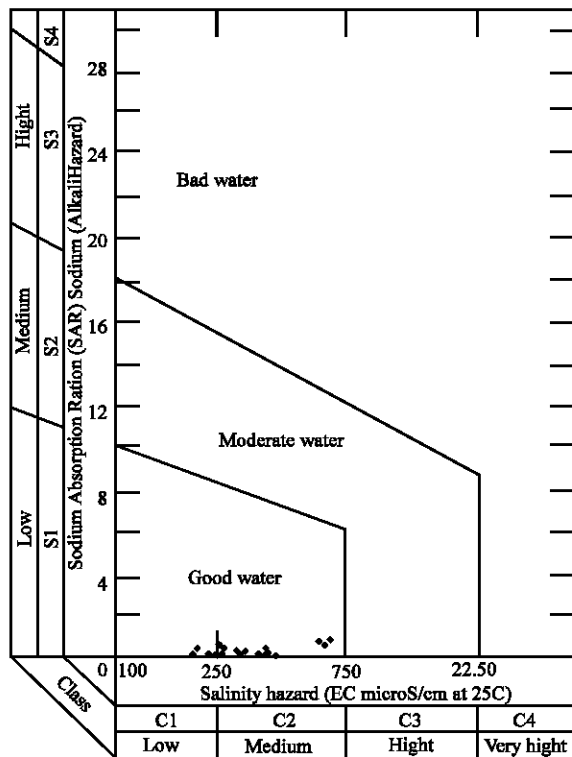


Fig. 7: Salinity and alkalinity hazard of irrigation water in US salinity diagram

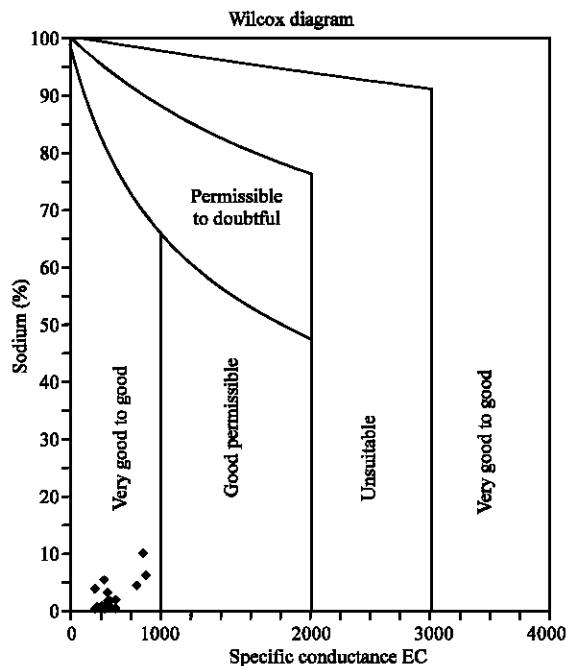


Fig. 8: Sodium percentages vs. EC plot (Wilcox, 1955)

(Table 6). The Wilcox (1955) diagram relating sodium percentage and total concentration (Fig. 8) shows that

most of the groundwater samples fall in the field of good to permissible. When the concentration of sodium is high in irrigation water, sodium ions tend to be absorbed by clay particles, displacing Mg^{2+} and Ca^{2+} ions. This exchange process of Na^+ in water for Ca^{2+} and Mg^{2+} in soil reduces the permeability and eventually results in soil with poor internal drainage. Hence, air and water circulation is restricted during wet conditions and such soils are usually hard when dry (Collins and Jenkins, 1996; Saleh *et al.*, 1999).

CONCLUSION

The hydrochemistry of groundwater varies in relation to different water-rock interactions (presence of calcite, dolomite and gypsum) and evaporation. Chemical analysis of some groundwater samples collected at different locations in the MengXu town basin showed that seven main types of groundwater such as $Ca-HCO_3-SO_4$, $Ca-HCO_3$ mainly and $Ca-HCO_3-SO_4-Cl$, $Ca-Mg-HCO_3$, $Ca-SO_4-HCO_3$, $Ca-Cl-HCO_3-NO_3$ are present within the study area. This study has demonstrated that the chemical composition of groundwater differs according to water types. In general, a significant increase in the degree of water mineralization was observed for the different water types. The least mineralized water is found closest to the main discharge area. The highest increase is observed in the concentration of the nitrate in the $Ca-HCO_3$ and $Ca-SO_4$ facies reflecting the degree of human influence. Dissolution of minerals, such as halite, gypsum, dolomite, calcite in the sediments results in the Cl^- , SO_4^{2-} , HCO_3^- , Na^+ , Ca^{2+} and Mg^{2+} content in the groundwater. Other reactions, such as cation exchange and the weathering of aluminosilicates, also contribute to the content of Na^+ and K^+ .

ACKNOWLEDGEMENT

The author wishes to thank Dr. Luo Zhao Hui (罗朝晖), Professor Wang (汪玉松) (CUG China), Abdu el Razzak and anonymous reviewer, whose critical comments greatly improved the manuscript.

REFERENCES

- Collins, R. and A. Jenkins, 1996. The impact of agricultural land use on stream chemistry in the middle Hills of the Himalayas. Nepal. J. Hydrol., 185: 71-86. DOI: 10.1046/j.1365-2427.2000.00608.
- Dixon, W. and B. Chiswell, 1992. The use of hydrochemical sections to identify recharge areas and saline intrusions in alluvial aquifers, southeast Queensland, Australia. J. Hydrol., 130: 299-338. DOI: 10.1016/0022-1694(92)90091-9.

- Drever, J.I., 1988. *The Geochemistry of Natural Waters*. 2nd Edn. Prentice Hall, Englewood. ISBN: 90-393-1852-2. DOI: 10.1016/0016-7037(82)90216-2.
- Edmunds, W.M., J.M. Cook, W.G. Darling, D.G. Kinniburgh, D.L. Miles, A.H. Bath, M. Morgan-Jones and J.N. Andrews, 1987. Baseline geochemical conditions in the chalk aquifer, Berkshire, UK: A basis for groundwater quality management. *Applied Geochem.*, 2: 251-274.
- Hidalgo, M.C. and J. Cruz-Sanjulian, 2001. Groundwater composition, hydro chemical evolution and mass transfer in a regional detrital aquifer (Baza basin, southern Spain). *Applied Geochem.*, 16: 745-758. DOI: 10.1016/S0883-2927(00)00078-0.
- Karanth, K.R., 1989. *Hydrogeology*. 2nd Edn. McGraw-Hill, New Delhi.
- Magaritz, M., A. Nadler, H. Koyumdjisky and N. Dan, 1981. The use of Na/Cl ratio to trace solute sources in a semiarid zone. *Water Resour. Res.*, 17: 602-608.
- Mathess, G., 1982. *The properties of groundwater*. Wiley, New York. DOI: 10.1016/0016-7037(82)90218-6.
- Meybeck, M., 1987. Global chemical weathering of surficial rocks estimated from river dissolved loads. *Am. J. Sci.*, 287: 401-428.
- Mohan, R., A.K. Singh, J.K. Tripathi and G.C. Chowdhary, 2000. Hydrochemistry and quality assessment of groundwater in Naini Industrial area, Allahabad District, Uttar Pradesh. *J. Geol. Soc. Ind.*, 55: 77-89.
- Parkhurst, D.L. and C.A.J. Appelo, 1999. Users guide to PHREEQC (version 2), a computer program for speciation, batch-reaction, one-dimensional transport and inverse geochemical calculations: U.S. Geological Survey Water Resources Investigations Report 99-4259. http://www.wrri.cr.usgs.gov/projects/GWC_coupled/phreeqc/html/final.html.
- Ragunath, H.M., 1987. *Groundwater*. Wiley Eastern Ltd, New Delhi, pp: 563.
- Ritcher, B.C. and W.C. Kreitler, 1993. *Geochemical techniques for identifying sources of groundwater salinization*. New York: CRC Press, ISBN: 1-56670-000-0.
- Saleh, A., F. Al-Ruwaih and M. Shehata, 1999. Hydrogeochemical processes operating within the main aquifers of Kuwait. *J. Arid. Environ.*, 42: 195-209. <http://www.ingentaconnect.com/content/ap/ae/1999/00000042/00000003/art00511>.
- Sami, K., 1992. Recharge mechanisms and geochemical processes in a semi-arid sedimentary basin, Eastern cape, South Africa. *J. Hydrol.*, 139: 27-48. DOI: 10.1016/0022-1694(92)90193-Y.
- Wilcox, L.V., 1955. *Classification and use of irrigation waters*. USDA, Circular 969, Washington, DC, USA.